

# Implementation of a P&E management system for a dual-source EV powered by different batteries

Mohan P. Thakre<sup>1</sup>, Pawan C. Tapre<sup>2</sup>, Sunil Somnath Kadlag<sup>3</sup>, Deepak Prakash Kadam<sup>4</sup>,  
Jayawant S. Thorat<sup>5</sup>, Rahul N. Nandeshwar<sup>5</sup>, Rohit S. Gaikwad<sup>6</sup>

<sup>1</sup>Department of Electrical Engineering, College of Engineering, Shri Vithal Education & Research Institute (SVERI's), Solapur, India

<sup>2</sup>Department of Electrical Engineering, SND College of Engineering Education & Research Center, Nashik, India

<sup>3</sup>Department of Electrical Engineering, Amrutvahini College of Engineering, Sangamner, India

<sup>4</sup>Department of Electrical Engineering, MET Institute of Engineering, Nashik, India

<sup>5</sup>Department of Electrical Engineering, K. K. Wagh Institute of Engineering Education and Research, Nashik, India

<sup>6</sup>Department of Electrical Engineering, Veermata Jijabai Technological Institute, Mumbai, India

## Article Info

### Article history:

Received Sep 25, 2022

Revised Nov 25, 2022

Accepted Jan 29, 2023

### Keywords:

Electric vehicles

Energy storage system

Hybrid energy storage system

Remaining useful life

Ultra-capacitor

## ABSTRACT

There is an era started in the field of power & energy (P&E) management in the electric vehicles (EVs) application cloud, which impacts the smart grid in significant ways and necessitates the collaboration of multiple branches of engineering. Most of the problems with EVs stem from their limited range, which can be improved by incorporating additional forms of energy storage. This paper makes an effort to bring a fresh viewpoint to the description of the power and energy management problem facing EV, taking into account all the needs of such a vehicle. Using a novel power and energy management system, the proposed methodology enables a systematic approach to this multidisciplinary problem. Implementing a power and energy management system for a dual-source EV using lead-acid batteries and ultra-capacitors (UCs) exemplifies the novel framework's capabilities. The electronic power development architecture is outlined in detail, along with the implementing modular blocks that make up the entire system architecture.

This is an open access article under the [CC BY-SA](https://creativecommons.org/licenses/by-sa/4.0/) license.



## Corresponding Author:

Mohan P. Thakre

Department of Electrical Engineering, College of Engineering, Shri Vithal Education & Research Institute  
Pandharpur, Solapur, Maharashtra, India

Email: mohanthakre@gmail.com

## 1. INTRODUCTION

According to the electric vehicles (EV) policy in India, car density is growing exponentially [1]. The application of EV has set a new era in the transportation field the recent innovations in the technologies applied in the storage system and motors [2]. Lower battery E density and driving ranges restricted to only hundreds of kilometres currently mesh a widespread use of electric cars. Many scientists and automotive industries are working on battery energy management to increase battery life, rapid recharging, price, and weight reduction [3]. Therefore, in battery-powered pure EV, the study focuses primarily on the concept of efficient energy storage [4]. The research was carried out to validate the novel energy storage system (ESS) topology using a multisource inverter. Work focusing on the intention of limiting battery peak current and weight, extending battery life, and increasing the driving range for plug-in EV, with the active-controlled parallel operation of a battery and an ultra-capacitor (UC) as energy devices [5]-[7].

A single-stage inverter connects the battery and UC to a three-phase load in the proposed architecture. Driving cycle torque demands reduce battery life due to load transient peak current [8]. UCs connected to dynamic response and traditional ESS meet transient load current demands. Battery and UC meet all load and

P exchange requirements managed by a multi-input innovative inverter [8], [9]. Driving requires long-term E and P. The battery supplies constant profile energy, while the UC supplies dynamic peak load profile. This ESS is cheaper and stronger than battery-based ones [10]. Hybrid energy storage system (HESS) power simulation (PSIM) uses closed-loop energy monitoring. Open-loop inverter control modes create power-sharing and a hardware prototype [11], [12]. Battery average current decreases standard case to 27%. The active power exchange between the propulsion system and the ESS extends the electric car's driving range [13], [14]. A hybrid remaining useful life (RUL) prediction model employing long short-term memory (LSTM) and Elman neural networks could monitor long-term battery degradation with higher cycle numbers and depict short-term capacity recovery at certain cycles [15].

The author examined lithium-ion battery thermal safety issues, including thermal behaviour, thermal runaway modelling, and battery pack security management rules, taking into account the heat manufacturing system and thermal battery characteristics [16]-[18]. Thermal runaway avoidance required heat, electrical, and mechanical model additives in numerous engineering techniques for material refining [19]-[21]. HESS optimization sizing the RUL. Peak current needs during transient load demands of the propulsion system degrade system quality and safety [22]. The author proposed a storage system with efficient E management using the SC and hybridization in E system [23]-[25]. Battery and UC power the electric car. Hybridization improves battery life. UC shares battery dynamic current stress, reducing current pulses a hybridization improves fuel economy 25-50% [22]-[25]. Section 2 provides an overview of the various types of EV and how they can be used in the context of contemporary control systems in the form of plug-in EV. In section 3, we model the various energy sources that go into an EV and compare them in terms of their energy density, power density, lifetime, cost, and weight. Before putting into action, the power-sharing capabilities of sources discovered in MATLAB and the PSIM environment, section 4 discusses the simulation study of the HESS. The study's findings are presented in section 5.

## 2. COMPARATIVE PERFORMANCE OF ENERGY SOURCES

EVs run on batteries. However, electric drive vehicle batteries possess limited life cycles, power density, charge-discharge rate, and charge time [26]. Batteries' discharge rate reduces energy delivery. Battery impedance raises temperature [27]. P storage system batteries are crucial. Transient loading challenges battery safety. Battery life is shortened by frequent charging and discharging without cell voltage balancing [26]-[29].

The ESS's battery-UC topology improved battery life, minimising the issues. High P density in the UC ensures proper energy and thermal management, enhancing EV efficiency [30]. Ragone plots compare energy source P and E density. This graphic shows that batteries have a higher E density than P density.

UC energy density is significantly lower than P density. UC's lifespan exceeds the batteries. UCs also offer better low-temperature properties than batteries. Ragone plot in Figure 1. Thus, battery-UC operating yields better outcomes. Battery and UC sources define all propulsion system driving cycle requirements. From the Ragone chart, UC has a high P density (6,800 W/kg) but a low E density. However, batteries have high E density (100 to 265 Wh/kg) and low P density. Thus, the combination outperforms each alone.

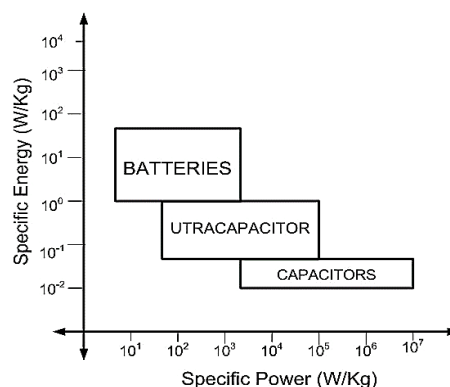


Figure 1. Ragone chart

## 3. MODELING OF SOURCES AND BATTERY

During the operation of an EV, the amount of energy that is stored in the storage system and the rate at which energy is extracted are the important factors that need to be considered in order to characterise the

energy management system. This is done in order to meet all of the specific energy demands and specific P demands that are imposed by driving cycles. In this section, the operation and modelling of a P source (UC), energy source (battery), and multisource inverter are broken down in detail, key terminology from the ESS is discussed.

### 3.1. Sources modelling

The internal resistance of source—the physical resistance of the electrolyte electrodes offers opposition to the flow of current, known as the internal resistance of the source, as shown in Figure 2. Operating temperature and the state of the charge depends upon the internal resistance of the energy source. The efficiency of a source can be improved by maintaining less internal resistance. Expression of Kirchhoff's voltage law to the equivalent circuit of source given by as (1):

$$V_{Bat} = V_o - I_{Bat} \cdot R_{int} \quad (1)$$

Where  $V_{Bat}$  is terminal voltage,  $R_{int}$  is internal resistance, and  $V_o$  is open circuit voltage (E.M.F).

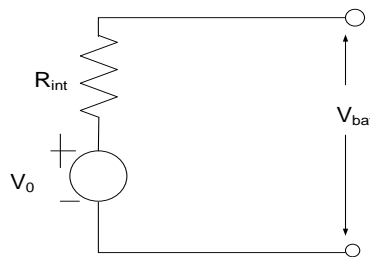


Figure 2. Internal resistance of sources

The ratio of discharge energy to the total mass of the battery is denoted as the specific energy of the battery as in (2). Actual energy extracted from the source depends upon discharge current and thus specific energy.

$$E_{sBat} = \frac{\text{Discharge Energy}}{\text{Total Mass of battery}} = \frac{E_{dis}}{M_{Bat}} \quad (2)$$

In (3) indicates the ratio of discharge P and mass of the battery is known as a specific P of the battery.

$$P_{sBat} = \frac{\text{Discharge Power}}{\text{Total Mass of battery}} = \frac{P_{dis}}{M_{bat}} \text{ W/kg} \quad (3)$$

This parameter also serves as a P level obtained from the battery. Battery capacity depends upon charges accumulated on the negative/positive electrode, which is measured in Coulombs (C) and expressed in terms of Ampere hour (Ah) (1 Ah=3,600 C). Energy capacity depends upon discharging current, presented in (4) with ' $C_{rate}$ '.

$$I_{c/dis} = k \cdot C_n \quad (4)$$

Where  $I_{c/dis}$  is charging/discharging current,  $C$  is battery capacity in Ah,  $k$  is multiplication factor of  $C$ , and  $n$  is  $C$  rate.

For example, a battery with 16 Ah for 10 hr discharge at a current of 8 Amp, is expressed as 0.5  $C_{10}$ . As  $C$ -rate increases,  $C$  decreases. Charge battery not used for a long period, the battery discharges by losing some amount of charges. Discharging of a cell depends upon the temperature of cells, the slow decomposition of electrodes, and the release of gas. This is expressed in percentage/24 hr shown in (5):

$$E_{SD} = \alpha_{SD} \cdot E_{BatNom} \quad (5)$$

Where  $\alpha_{SD}$  is coefficient of self-discharge for 24 hr, and  $E_{BatNom}$  is nominal energy capacity in Wh. In (6) shows the ratio of Ah discharge to complete recharge:

$$Effi_{Ah} = \frac{Ah(\text{Discharge})}{Ah(\text{complete recharge})} \quad (6)$$

Useful to compare various types of energy sources. Battery energy efficiency is defined as the ratio of energy delivered from a particular state of charge (SOC) to energy consumed to maintain the same SOC. Higher battery efficiency is obtained by limiting rapid P discharges.

### 3.2. Battery modelling

For a discharge time  $t_{dis}$ , the battery discharge energy  $E_{dis}$ , shown in (7) which is a function of open-circuit voltage (E.M.F.)  $V_o$ , with internal resistance  $R_{int}$  and constant discharge current  $I_{con}$ .

$$E_{dis} = \int_0^t P_{Bat}(t) \cdot dt = t_{dis}(V_o - I_{Bat} \cdot R_{int})I_{con} \quad (7)$$

Battery charging time was selected as  $t_{dis} = t_{crg}$  with the same magnitude of discharging current  $I_{con}$  and battery discharge energy  $E_{crg}$  shown in (8):

$$E_{crg} = \int_0^t |P_{Bat}|(t) \cdot dt = t_{crg}(V_o + |I_{Bat}| \cdot R_{int})|I_{con}| \quad (8)$$

Battery efficiency is expressed as the ratio of discharging energy to the charging energy shown in (9):

$$n_{Bat} = \frac{E_{dis}}{E_{crg}} = \frac{(V_o - |I_{Bat}| \cdot R_{int})}{(V_o + |I_{Bat}| \cdot R_{int})} \quad (9)$$

In 1897 W. Peukert formulated empirical relation between capacity (Q), discharging current (I), and time (t) shown in (10):

$$I^n \cdot t_{cut} = \lambda \quad (10)$$

Where I is discharge current,  $t_{cut}$  is time taken to reach the satisfactory voltage, n is curve fitting constant (n is 1 small currents, n is 2 large currents).

The relation can be derived as in (11):

$$Q = I \cdot t_{cut} \quad (11)$$

From (11) we can form discharge current in (12):

$$I^n \cdot \frac{Q}{I} = \lambda \quad (12)$$

In (13) indicates, battery SoC corresponds to real-time battery capacity (remaining capacity):

$$SoC(t) = Q - \int_0^t i(\tau) \cdot d\tau \quad (13)$$

In (14) indicates, state of discharge (SoD) is:

$$SoD(t) = \int_0^t i(\tau) \cdot d\tau \quad (14)$$

Battery capacity can be expressed in another way called Depth of discharge as in (15):

$$DoD(t) = \frac{Q - SoC(t)}{Q} \cdot 100\% = \frac{i(\tau) \cdot d\tau}{Q} \quad (15)$$

By deriving  $DoD(t)$  obtained as in (16):

$$DoD(t) = \frac{SoD}{Q_T} \quad (16)$$

The more practical equation to calculate discharge time obtained from manufacturers is given as in (17):

$$T = \frac{C \left[ \frac{C}{h} \right]^{n-1}}{I^n} \quad (17)$$

Where C is nominal capacity, h is hour rating, I is discharge current, and battery capacity in (Ah) is  $T \cdot I$ , practically SoC obtained by (18):

$$SoC_{Bat}(k+1) = SoC_{Bat}(k) + \frac{I_{con} \Delta T}{C_n 3600} \quad (18)$$

In hybrid source energy management systems UC modeling is very important to optimize the size of the storage system.

### 3.3. Maximum discharging power

Multiplication of maximum discharging current and minimum allowable voltage gives the value of maximum discharging P. Maximum discharging P due to current expressed as in (19):

$$P_{disMax} = |I_{batMax}|(V_o) - |I_{BatMax}|^2 \cdot (R_{int}) \text{ with the same SoC} \quad (19)$$

Maximum discharging P as given in (20):

$$P_{disMax} = V_{BatMin} \left[ \frac{V_o - V_{Batmin}}{R_{int}} \right] \quad (20)$$

Where  $V_{BatMin}$  is the minimum allowable voltage.

### 3.4. Maximum charging power

In (21) indicates maximum charging P which depends upon maximum charging voltage and current. Charging rates always maintained less than the charge accumulation rate.

$$P_{crgMax} = |I_{batMax}|(V_o) + |I_{BatMax}|^2 \cdot (R_{int}) \text{ with the same SoC.}$$

$$P_{crgMax} = V_{BatMax} \left[ \frac{V_{Batmax} - V_o}{R_{int}} \right] \quad (21)$$

$$V_{BatMax} = \text{maximum charging voltage}$$

Using cell balancing overcharging of the cell is prevented. By limiting maximum charging P, the life of the cell will be extended.

## 4. RESULT AND DISCUSSION

Steps involve modeling and simulating any system, i.e., representing the system with mathematical relationships, finalizing variables of input and output, selecting the correct model, and interpreting and validating the system. To comprehend the UCs charging and discharge features and electrical behavior, a simulation is conducted as follows in the MATLAB and PSIM environment. To validate the UCs dynamic behavioral response, the simulation is conducted in MATLAB/Simulink software, where the battery is attached directly to the DC link, and the UC is connected to the DC link via a dc/dc converter. A simulation for DC/DC converter based on UC/battery design has been chosen to recognize the fundamental significance of hybridization. In this design, current sharing is observed with the gradually increased resistive load over time. Batteries (12 V ( $V_B$ ), 50 Ah) are chosen with a UC of 12 V ( $V_U$ ), 20 Farad. With time delays, three resistive loads are gradually added and connected for loading purposes, and control switches are equipped for low charge protection. The model shown in Figure 3 is achieved in MATLAB/Simulink from the Simscape tool. The total simulation time is selected as 1,000 s.

For different time steps the resistive load gradually enters the circuit. The UC (12 Farad) and the battery share the peak load during the dynamic load variation. The outcome shown that the discharge of the battery begins at 320 sec. with a tiny decrease in the voltage of the battery owing to the internal battery resistance; the current is 2 A. UC shares the dynamic shift in load demand, thus preserving the DC link voltage by restricting the current of the battery. In simulink model, it is seen that the UC provides the peak P (at  $t=300$  s) that limit the battery currently in the event of dynamic peak P need of the load as shown in Figure 4.

The PSIM simulation comprises an ac load such as induction motor (IM) fed inverter as shown in Figure 5, in which the suggested novel inverter is connected to an AC link. The source of the battery 24 V is linked to the inverter-1, while the UC (300 Farad, 24 volts) is attached to the inverter-2. The results demonstrate the P-sharing behavior of the battery and UC during a dynamic change in load.

Using a simulation of the PSIM script file, a space vector analogy is used. Control signals are acquired using the script control block. Current and torque feedback is obtained from the sensors. As an optimal battery and UC, the DC sources are chosen for simulation. A multi-source hybrid inverter is designed with insulated gate bipolar transistors (IGBTs) based on semiconductors. A 3-ph IM characterizes the load. Since the IM itself is the balanced RL load, the current sensor senses from one of the phases; taco generator is also used to sense the shaft speed. The selected period of simulation is 2 sec.

This simulation demonstrates active and reactive (P-Q) load control. In view of the inductive load (RL), the motor's P factor lags. The outcomes denote the P&Q requirements of the load.

- a. Positive P is the power injected into the load from the DC bus.
- b. In Var, Q with positive magnitude is Q being injected into the load.
- c. In any combination where negative magnitudes inject P and Q from the load into the DC bus, bidirectional P flow is possible.

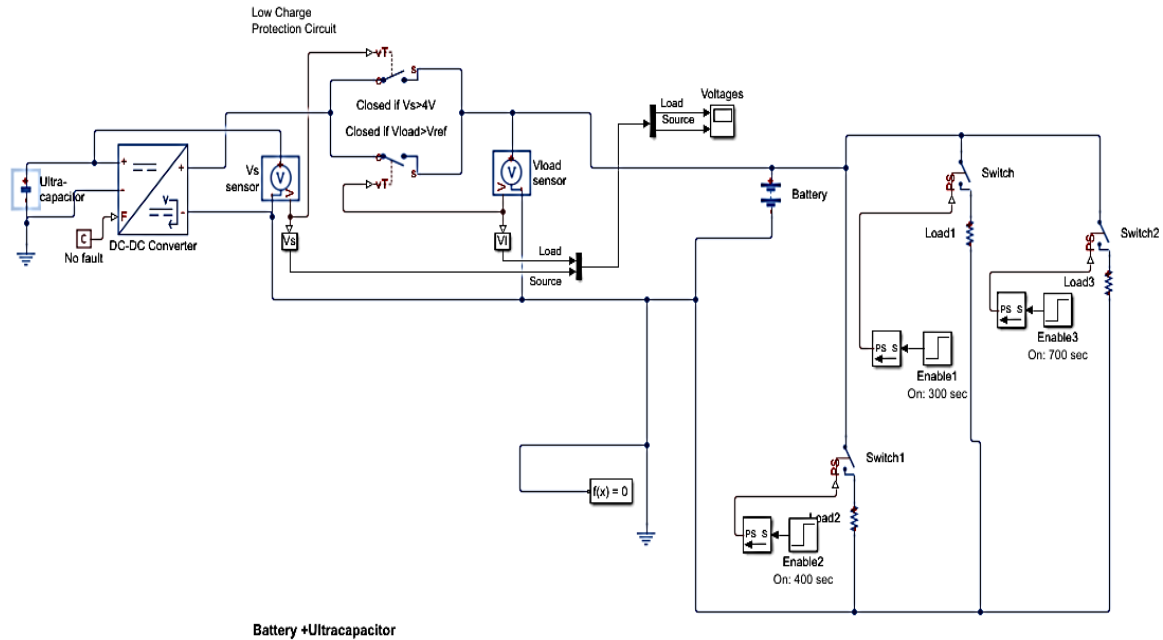


Figure 3. Simulink model of the energy management system

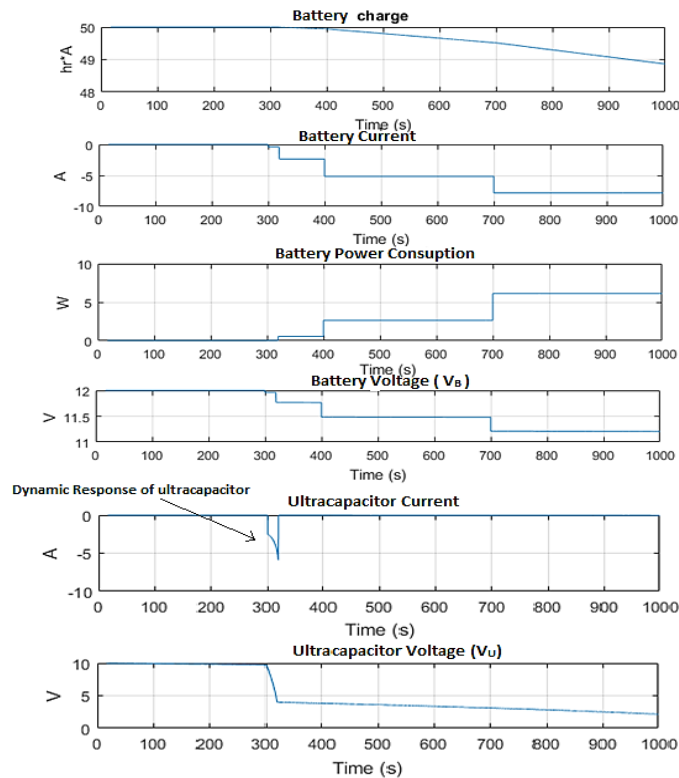


Figure 4. Study system outcome of various parameter

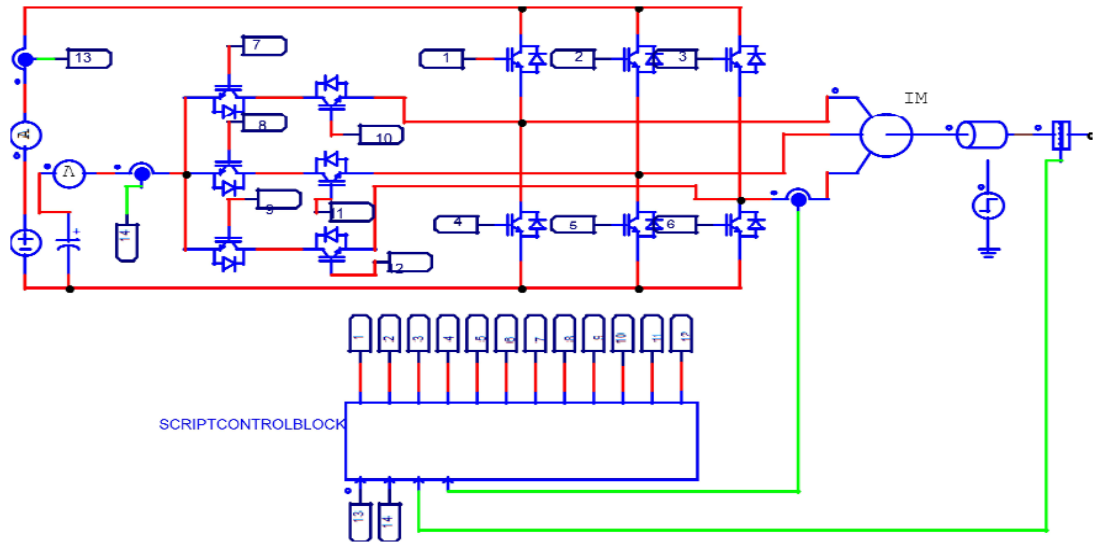
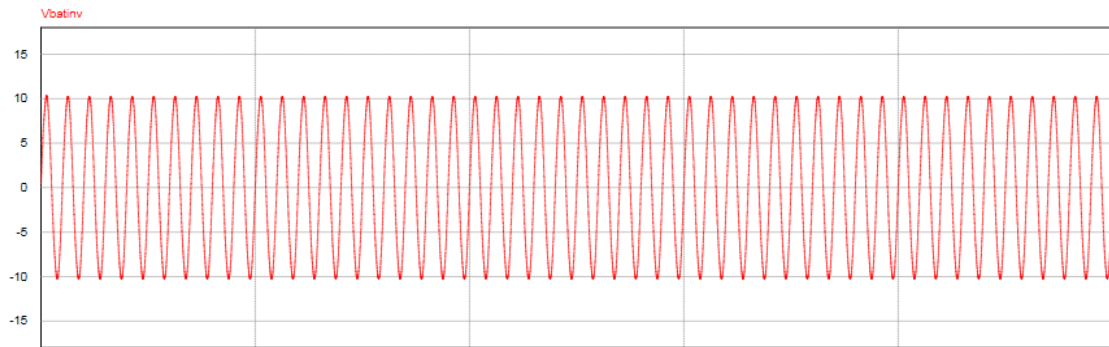


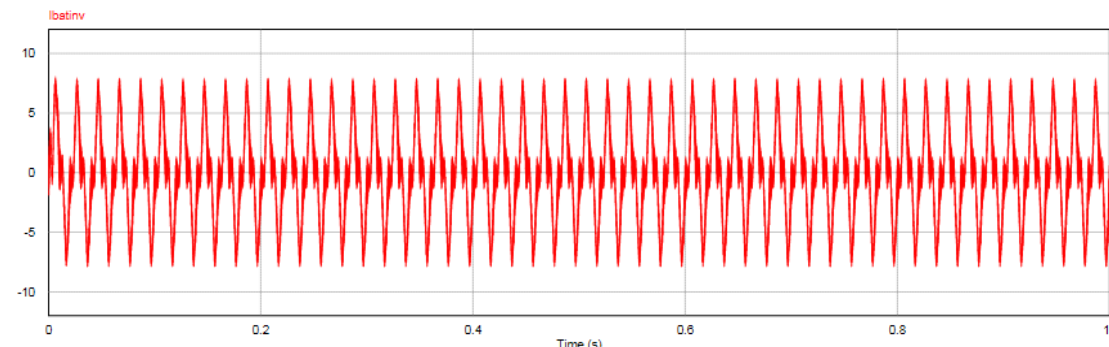
Figure 5. Hybrid converter model considering load

**4.1. Mode-1 (battery & load)**

In this mode, battery drives the load and an UC is not used. Battery connected to the inverter, which converts DC to AC and drives the load alone. Battery current and voltage are measured with scope. In Figures 6(a) and (b) are shown inverter-1 output voltage and current respectively. In mode-1 of Figure 6, the motor is supplied by a 24 V battery via an inverter. To get these findings, we run a 1 s model of inverter mode. As such an outcome of evidence suggesting that the P is in the positive direction of the graph, P and Q are supplied into the motor as indicated in Figures 7(a) and (b). Mode-2 is nomenclature as mixed mode, where the P is supplied to the motor by the battery (energy requirement) and UC (P requirement) via an inverter.



(a)



(b)

Figure 6. Inverter 1 findings for for mode-1 (supplied through battery alone); (a)  $V_{out}$  inverter-1 and (b)  $I_{out}$  inverter-1

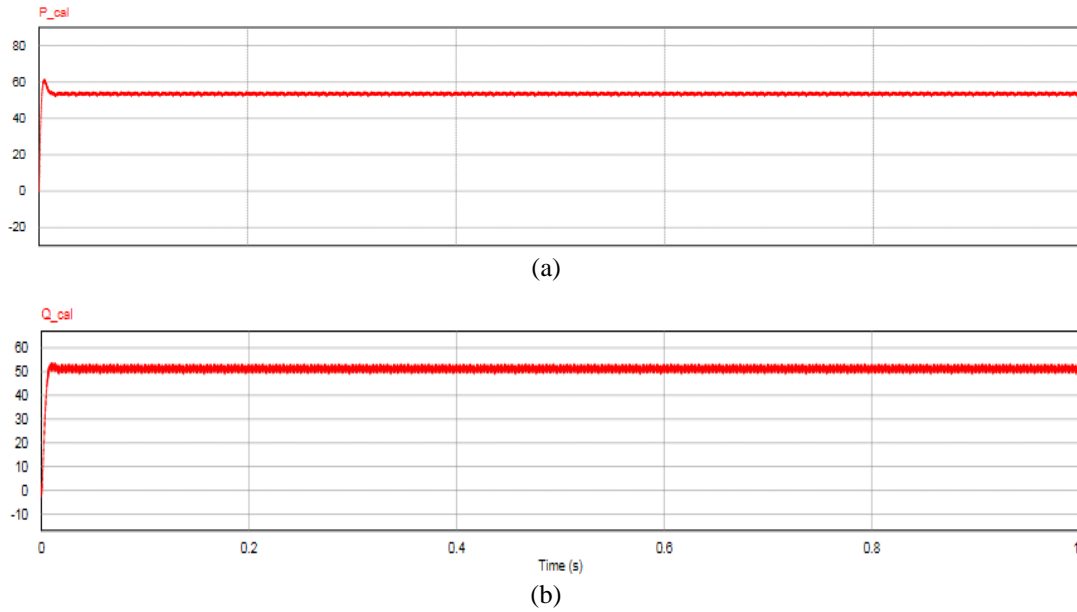


Figure 7. P and Q used up in mode 1 utilization; (a) P and (b) Q

**4.2. Mode-2 (battery, UC & load)**

In this mode, battery drives the load by charging the UC. The effective output voltage is equal to  $(V_B - V_U)$ . Computation is 1 sec. Various loading reference increment at 0.3 sec. UCs share peak P demand due to their quick P dynamics, reducing current stress during peak P demand. Figures 8(a) and (b) shows inverter-1's voltage and current output.

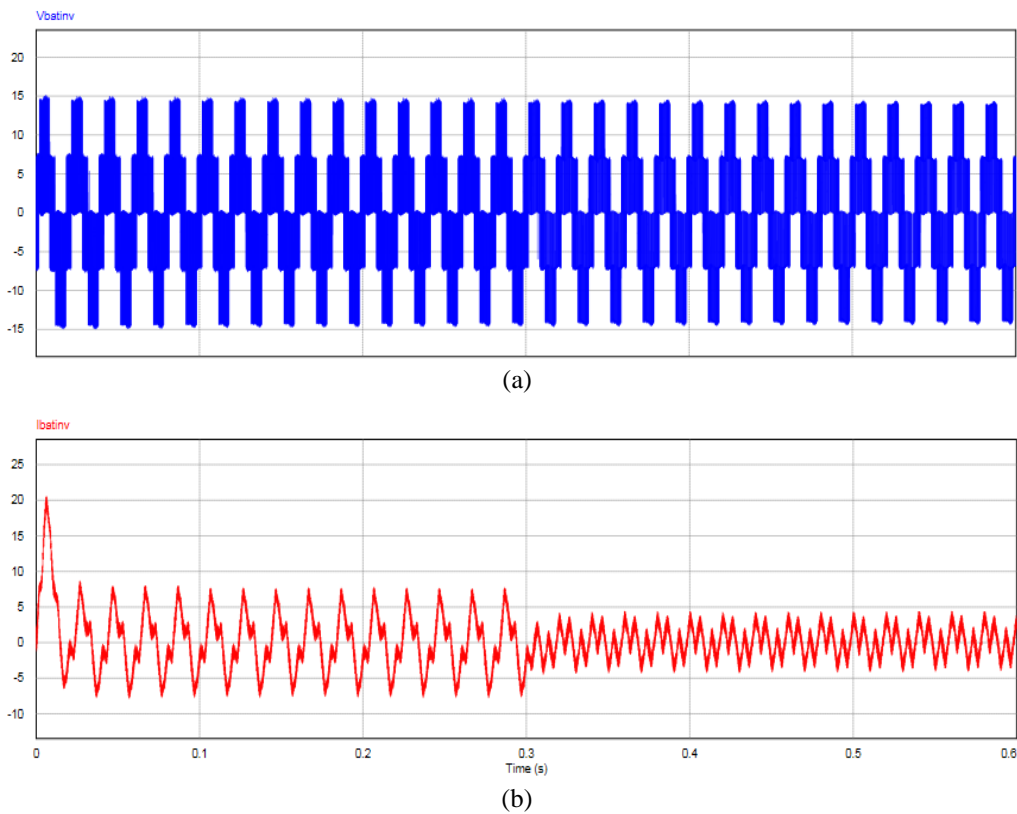


Figure 8. Inverter-1 voltage and current output; (a) inverter-1 (battery connected) voltage and (b) inverter-1 (battery connected) current



Figure 9 shows the UC terminal voltage waveform, it is evident that the UC gets discharged in load at 0.3 sec. Current stress on the battery is shared by the UC. Comparative analysis between reference and calculated active and reactive P was indicated with the help of Figures 10(a) and (b). The steady-state 3-axis ABC frame being transformed into a 2-axis dynamic dq frame to govern P-sharing from sources to loads. The UC and battery P the load during simulation.

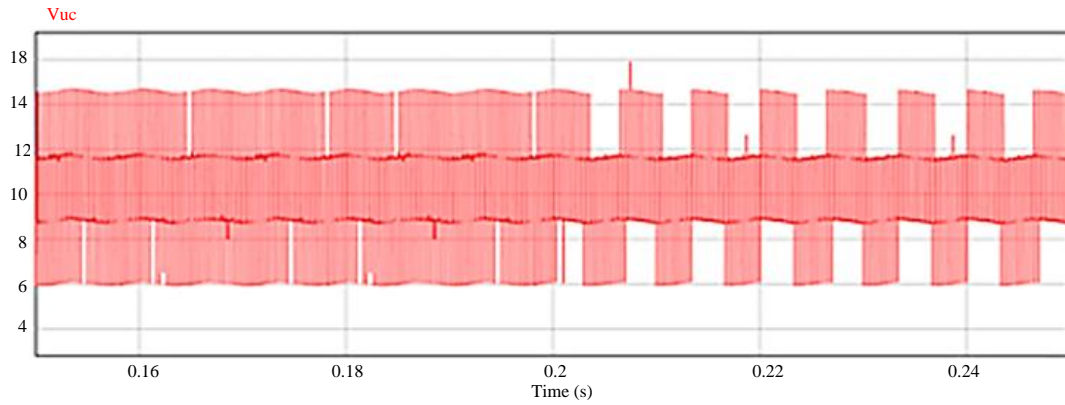
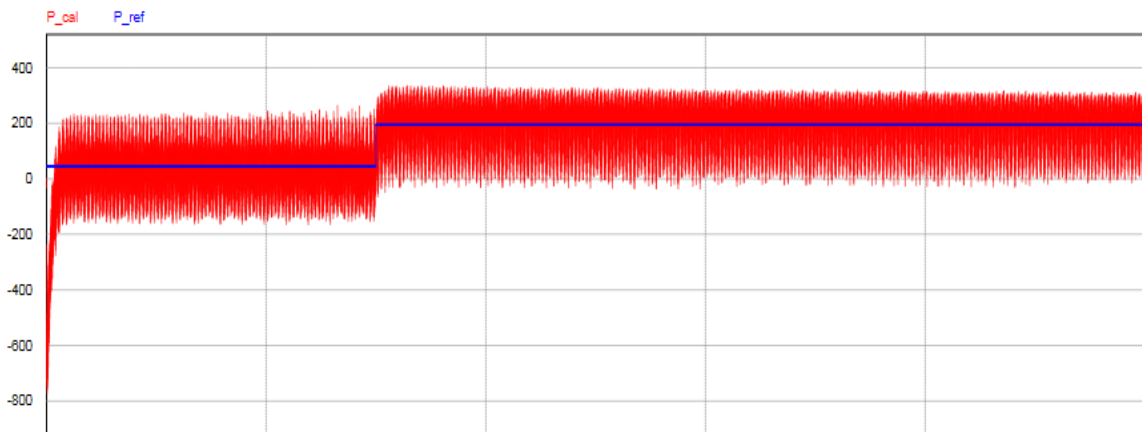
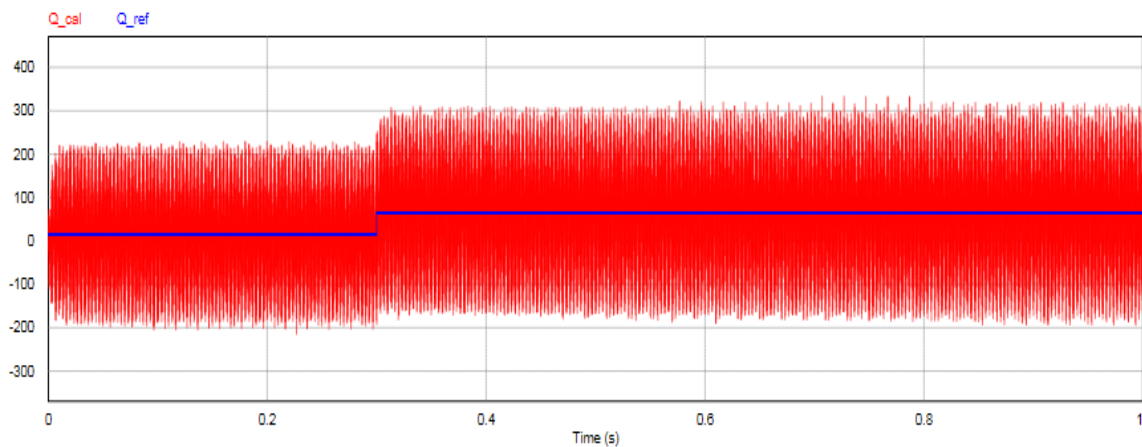


Figure 9. Terminal voltage of UC  $V_{UC}$  during dynamic P requirement 0.3 sec



(a)



(b)

Figure 10. Reference vs calculated; (a) P and (b) Q

## 5. CONCLUSION

Attributable to these simulation results, a feasible hybrid (multisource) inverter topology for HESS has been proposed. One key benefit of this topology is that no intermediate stages are required between the P grid/motor and the energy storage units. The efficiency of EV can be increased through the use of a novel multisource connection that better fulfils the load's P demand. Smooth current sharing and reduced average currents are additional benefits of using a multisource inverter. On the other hand, an ESS can increase its efficiency by cutting down on the size and cost of the converter by having the battery directly drive the load (a motor/power system) without performing a boost operation. THE SVPWM-based control strategy allows for P&E transfer between multiple sources during the dynamic load demands of the driving cycle, which increases load power stability.




## REFERENCES

- [1] C. Cosgrove, "Energy consumption in GCC countries. Power on, power up," in *2017 4th IEEE International Conference on Engineering Technologies and Applied Sciences (ICETAS)*, pp. 1-6, Nov. 2017, doi: 10.1109/icetas.2017.8277862.
- [2] H. Abubakr, J. C. Vasquez, K. Mahmoud, M. M. F. Darwish, and J. M. Guerrero, "Comprehensive Review on Renewable Energy Sources in Egypt—Current Status, Grid Codes and Future Vision," *IEEE Access*, vol. 10, pp. 4081–4101, 2022, doi: 10.1109/access.2022.3140385.
- [3] A. Mehrabani, H. Mardani, and M. S. Ghazizadeh, "Optimal Energy Management in Smart Home Considering Renewable Energies, Electric Vehicle, and Demand-Side Management," in *2022 9th Iranian Conference on Renewable Energy & Distributed Generation (ICREDG)*, pp. 1-5, Feb. 2022, doi: 10.1109/icredg54199.2022.9804525.
- [4] R. R. Jha, A. Dubey, T. Hong, and D. Zhao, "Distributed Algorithm for Volt - VAR Optimization in Unbalanced Distribution System," in *2020 IEEE Power & Energy Society Innovative Smart Grid Technologies Conference (ISGT)*, pp. 1-5, Feb. 2020, doi: 10.1109/isgt45199.2020.9087698.
- [5] Y. Zhang, X. Wang, J. Wang, and Y. Zhang, "Deep Reinforcement Learning Based Volt-VAR Optimization in Smart Distribution Systems," *IEEE Transactions on Smart Grid*, vol. 12, no. 1, pp. 361–371, Jan. 2021, doi: 10.1109/tsg.2020.3010130.
- [6] X. Li and S. Wang, "Energy management and operational control methods for grid battery energy storage systems," *CSEE Journal of Power and Energy Systems*, vol. 7, no. 5, pp. 1026–1040, Sep. 2021, doi: 10.17775/CSEEJPES.2019.00160.
- [7] F. A. Asuhaimi, J. P. B. Nadas, and M. A. Imran, "Delay-optimal mode selection in device-to-device communications for smart grid," in *2017 IEEE International Conference on Smart Grid Communications (SmartGridComm)*, pp. 26-31, Oct. 2017, doi: 10.1109/smartgridcomm.2017.8340710.
- [8] A. Sendin, J. Matanza, and R. Ferrus, "Smart Grid Applications and Services," in *Smart Grid Telecommunications: Fundamentals and Technologies in the 5G Era*, IEEE, 2021, pp. 137–177, doi: 10.1002/9781119755401.ch5.
- [9] A. Ostadi and M. Kazerani, "A Comparative Analysis of Optimal Sizing of Battery-Only, Ultracapacitor-Only, and Battery–Ultracapacitor Hybrid Energy Storage Systems for a City Bus," *IEEE Transactions on Vehicular Technology*, vol. 64, no. 10, pp. 4449–4460, Oct. 2015, doi: 10.1109/tvt.2014.2371912.
- [10] B. Chen, L. Chen, Y. Tan, and X. Kuang, "Investigations on Communication and Management Techniques for Electric Internet of Things Applications in Smart Grid," in *2021 China International Conference on Electricity Distribution (CICED)*, pp. 515-518, Apr. 2021, doi: 10.1109/ciced50259.2021.9556838.
- [11] S. Dusmez and A. Khaligh, "A Supervisory Power-Splitting Approach for a New Ultracapacitor–Battery Vehicle Deploying Two Propulsion Machines," *IEEE Transactions on Industrial Informatics*, vol. 10, no. 3, pp. 1960–1971, Aug. 2014, doi: 10.1109/tii.2014.2299237.
- [12] J. Bhatt, O. Jani, and V. S. K. V. Harish, "Wireless Communication Technologies for Indian Smart Grid: Fitness Evaluation and Optimal Decision-making," in *2021 9th IEEE International Conference on Power Systems (ICPS)*, pp. 1-6, Dec. 2021, doi: 10.1109/icps52420.2021.9670197.
- [13] F. J. Lin, B.-Y. Chen, B.-T. Lin, and W.-H. Hu, "Charging architecture for M2M communications," in *2016 IEEE 3rd World Forum on Internet of Things (WF-IoT)*, Dec. 2016, doi: 10.1109/wf-iot.2016.7845405.
- [14] Z. Fan, R. Haines, and P. Kulkarni, "M2M communications for E-health and smart grid: an industry and standard perspective," *IEEE Wireless Communications*, vol. 21, no. 1, pp. 62–69, Feb. 2014, doi: 10.1109/mwc.2014.6757898.
- [15] A. K. Farraj, E. M. Hammad, A. A. Daoud, and D. Kundur, "A game-theoretic control approach to mitigate cyber switching attacks in Smart Grid systems," in *2014 IEEE International Conference on Smart Grid Communications (SmartGridComm)*, pp. 958-963, Nov. 2014, doi: 10.1109/smartgridcomm.2014.7007772.
- [16] O. P. Taiwo, R. Tiako, and I. E. Davidson, "An improvement of voltage unbalance in a low voltage 11/0.4 kV electric power distribution network under 3-phase unbalance load condition using dynamic voltage restorer," in *2017 IEEE PES PowerAfrica*, pp. 126-131, Jun. 2017, doi: 10.1109/powerafrica.2017.7991211.
- [17] I. A. Ibrahim and M. J. Hossain, "Low Voltage Distribution Networks Modeling and Unbalanced (Optimal) Power Flow: A Comprehensive Review," *IEEE Access*, vol. 9, pp. 143026–143084, 2021, doi: 10.1109/access.2021.3120803.
- [18] C. Jian, L. Yutian, and B. Guannan, "Optimal operating strategy for distribution networks with PV and BESS considering flexible energy storage," in *2016 IEEE Power and Energy Society General Meeting (PESGM)*, pp. 1-5, Jul. 2016, doi: 10.1109/pesgm.2016.7741131.
- [19] M. Mathur, R. Pradhan, and P. Jena, "Control of AC-DC Hybrid Microgrid in the Presence of BESS and a Scheme to Limit Sudden Power Transfer," in *2022 Second International Conference on Power, Control and Computing Technologies (ICPC2T)*, pp. 1-6, Mar. 2022, doi: 10.1109/icpc2t53885.2022.9776913.
- [20] M. P. Thakre and P. S. Borse, "Analytical Evaluation of FOC and DTC Induction Motor Drives in Three Levels and Five Levels Diode Clamped Inverter," in *2020 International Conference on Power, Energy, Control and Transmission Systems (ICPECTS)*, pp. 1-6, Dec. 2020, doi: 10.1109/icpects49113.2020.9337015.
- [21] A. Jawad, Nahid-Al-Masood, and S. Munim, "Optimal Sizing of BESS for Attaining Frequency Stability Under High PV Penetration," in *2021 International Conference on Technology and Policy in Energy and Electric Power (ICT-PEP)*, pp. 348-353, Sep. 2021, doi: 10.1109/ict-pep53949.2021.9601074.




- [22] H. Khajeh, C. Parthasarathy, and H. Laaksonen, "Effects of Battery Aging on BESS Participation in Frequency Service Markets–Finnish Case Study," in *2022 18th International Conference on the European Energy Market (EEM)*, pp. 1-6, Sep. 2022, doi: 10.1109/eem54602.2022.9921139.
- [23] M. Thakre, J. Mane, and V. Hadke, "Performance Analysis of SRM Based on Asymmetrical Bridge Converter for Plug-in Hybrid Electric Vehicle," in *2020 International Conference on Power, Energy, Control and Transmission Systems (ICPECTS)*, pp. 1-6, Dec. 2020, doi: 10.1109/icpepts49113.2020.9337059.
- [24] P. K. Chowdhary and M. P. Thakre, "MMC-Based SRM Drives for Hybrid-EV with Decentralized BESS in Battery Driving Mode," in *2020 International Conference on Power, Energy, Control and Transmission Systems (ICPECTS)*, pp. 1-6, Dec. 2020, doi: 10.1109/icpepts49113.2020.9337029.
- [25] Z. Wang, K. Chu, B. Liu, and M. Cheng, "Three-port high-frequency transformer based current-source electric drive system for hybrid electric vehicles," in *2015 IEEE Magnetics Conference (INTERMAG)*, p. 1, May 2015, doi: 10.1109/intmag.2015.7156892.
- [26] J. A. Mane, M. R. Rade, and M. P. Thakre, "Significant Affect of EV Charging on Grid with Renewable Technologies," in *International Conference on Smart Data Intelligence (ICSMDI 2021)*, 2021, pp. 1-8, doi: 10.2139/ssrn.3852716.
- [27] M. Shahverdi, M. S. Mazzola, Q. Grice, and M. Doude, "Bandwidth-Based Control Strategy for a Series HEV With Light Energy Storage System," *IEEE Transactions on Vehicular Technology*, vol. 66, no. 2, pp. 1040–1052, Feb. 2017, doi: 10.1109/tvt.2016.2559949.
- [28] M. Passalacqua, D. Lanzarotto, M. Repetto, L. Vaccaro, A. Bonfiglio, and M. Marchesoni, "Fuel Economy and EMS for a Series Hybrid Vehicle Based on Supercapacitor Storage," *IEEE Transactions on Power Electronics*, vol. 34, no. 10, pp. 9966–9977, Oct. 2019, doi: 10.1109/tpe.2019.2895209.
- [29] M. P. Thakre and N. Kumar, "Design, Development, and Simulation Modeling of Hybrid Electric Vehicles Incorporating with BLDC Drive," in *Energy Systems in Electrical Engineering*, Springer Nature Singapore, 2022, pp. 513–551, doi: 10.1007/978-981-19-0979-5\_20.
- [30] M. Shahverdi, M. S. Mazzola, Q. Grice, and M. Doude, "Pareto Front of Energy Storage Size and Series HEV Fuel Economy Using Bandwidth-Based Control Strategy," *IEEE Transactions on Transportation Electrification*, vol. 2, no. 1, pp. 36–51, Mar. 2016, doi: 10.1109/tte.2015.2508000.

## BIOGRAPHIES OF AUTHORS






**Dr. Mohan P. Thakre**    received the B.Tech. and M.Tech. degrees in electrical power engineering from Dr. Babasaheb Ambedkar Technological University (Dr. BATU), Maharashtra, India, in 2009 and 2011 respectively, and the Ph.D. degree in electrical engineering from Visvesvaraya National Institute of Technology (VNIT), Nagpur, Maharashtra, India in 2017. Currently, he is an Associate Professor at the Department of Electrical Engineering, College of Engineering, Shri Vithal Education & Research Institute, Pandharpur, Maharashtra, India. His research interests include FACTS and power system protection. He can be contacted at email: mohanthakre@gmail.com.






**Dr. Pawan C. Tapre**    received the B.E. and M.E. degrees in Electrical Power System Engineering from Sant Gadge Baba Amravati University (SGBAU), Maharashtra, India, in 1995 and 2002 respectively, and a Ph.D. degree in Electrical Engineering from Dr. C.V. Raman University (Dr. CVRU), Bilaspur, Chhattisgarh, India in 2022. Currently, he is an Assistant Professor at the Department of Electrical Engineering, S.N.D. College of Engineering and Research Center, Yeola (Nashik), Maharashtra, India. His research interests include deregulated power systems, FACTS, power systems, and power system protection. He can be contacted at email: pawan.tapre73@gmail.com.






**Dr. Sunil Somnath Kadlag**    received B.E. in Electrical Engineering from received B.E in Electrical Engineering from Dr. Babasaheb Ambedkar Marathawada University (Dr. BAMU), Aurangabad in 1997 and M.E. in Electrical Engineering (Control System) from Government College of Engineering Pune (Pune University) in 2005 and Ph.D. in Electrical Engineering from Suresh Gyan Vihar University Jaipur (Rajasthan) in 2021. His research area is electric vehicles. He is presently working as an Associate Professor and Head of the Department of Electrical Engineering, Amrutvahini College of Engineering Sangamner, Savitribai Phule Pune University, Pune, Maharashtra, India. He can be contacted at email: sunilkadlag5675@gmail.com.






**Dr. Deepak Prakash Kadam**    received a B.E. from the Government College of Engineering, Amaravati, and M.E. degrees in electrical power systems from Walchand College of Engineering, Sangli, Maharashtra, India, in 1997 and 2005 respectively, and the Ph.D. degree in electrical engineering from Savitribai Phule Pune University, Pune Maharashtra, India in 2015. Currently, he is an Associate Professor at the Department of Electrical Engineering, Bhujbal Knowledge City, MET Institute of Engineering, Nashik, India. His research interests include renewable energy technology, power quality, and power system. His total teaching experience is around 23 years. He can be contacted at email: dpkadam@gmail.com.






**Mr. Jaywant S. Thorat**    received the B.E.(Electrical ) from Govt. College of Engineering Karad, Maharashtra, India in 1992. Presently he is appearing M.E. (Electrical Power System) from K. K. Wagh Institute of Engineering Education & Research, Nashik, Maharashtra, India. Currently, he is Head of Research & Development at Vision Vidyut Engineers Pvt. Ltd. Thane, Maharashtra, India. His research interest includes medium voltage electrical equipments and electrical power distribution system. He can be contacted at email: jaywant@visionvidyut.com.



**Rahul N. Nandeshwar**    received the B.E. degree in Electrical Engineering from RTM Nagpur University in 2015 and M.E. in Electrical Power System from Savitri Bai Phule Pune University, Maharashtra, India, in 2023. Currently, he is senior electrical engineer at currency note press, his research interests include power system protection and non-conventional energy sources. He can be contacted at email: rahul.07narendra@gmail.com.



**Rohit S. Gaikwad**    received a B.E. in Electrical Engineering from MET Institute of Engineering, Nasik and an M.Tech. degree in Power Systems from VJTI, Mumbai, Maharashtra, India, in 2019 and 2022, respectively. His research interests include power system protection, smart grid, and PHEV. He can be contacted at email: rohitskumar601@gmail.com.